www.sciencemag.org/content/360/6394/1227/suppl/DC1

Supplementary Materials for

Synapse-specific representation of the identity of overlapping memory engrams

Kareem Abdou*, Mohammad Shehata*, Kiriko Choko, Hirofumi Nishizono, Mina Matsuo, Shin-ichi Muramatsu, Kaoru Inokuchi†

*These authors contributed equally to this work.
†Corresponding author. Email: inokuchi@med.u-toyama.ac.jp

Published 15 June 2018, *Science* **360**, 1227 (2018)
DOI: 10.1126/science.aat3810

This PDF file includes:

Materials and Methods

Animals

Naive male C57BL/6J (purchased from Sankyo Labo Service Co. Inc., Tokyo, Japan) and c-Fos::tTA transgenic mice (Mutant Mouse Regional Resource Center, stock number: 031756-MU) were obtained as described previously (*11*, *16*). The R26R::H2B-mCherry transgenic mice (CDB0204K) have been described previously (*29*). The progeny for the c-Fos::tTA and c-Fos::tTA/R26R::H2B-mCherry double transgenic mouse lines were generated using *in vitro* fertilization with eggs from C57BL/6J mice and embryo transfer techniques. These transgenic mice were raised on food containing 40 mg kg^{-1} DOX and maintained on Dox pellets except for 2 days before the conditioning session. All mice were maintained on a 12 h light/dark cycle at 24°C ± 3°C and 55% ± 5% humidity, had access to food and water *ad libitum*, and were housed with littermates until surgery. Mice for behavioural analyses were 12–18 weeks old. All procedures involving the use of animals were performed in accordance with the guidelines of the National Institutes of Health (NIH) and were approved by the Animal Care and Use Committee of the University of Toyama and the Institutional Committee for the Care and Use of Experimental Animals of Jikei University.

Viral constructs

The recombinant AAV vectors used were AAV-TRE_{3G}-Cre and AAV-hSyn1-DIO-oChIEF-Citrine at a 1:10 ratio. The pAAV-hSyn1-DIO-oChIEF-Citrine plasmid was acquired from Addgene (Addgene plasmid 50973). For pAAV-TRE_{3G}-Cre preparation, pAAV-TRE_{3G}-$CreER^{T2}$ was first constructed by replacement of the PCR-amplified TRE_{3G}-$CreER^{T2}$ of pLenti-TRE_{3G}-$CreER^{T2}$, which has been described previously (*18*), with primers (sense, GCGACGCGTCGAATTCGTCTTCAAGAATTCCTC; antisense, CAGGCCGCGGGAAGGAAG) into pAAV-EF1a-DIO-EYFP (donated by Dr K. Deisseroth) at the *Mlu*I-*Sac*II restriction sites. Then, inverse PCR was performed using the pAAV-TRE_{3G}-$CreER^{T2}$ template with primers (sense, GGATCATCCATCCATCACAGTGGC; antisense, TTAATCGCCATCTTCCAGCAGGCG) to construct pAAV-TRE_{3G}-Cre. The recombinant AAV vectors were produced as described previously (*30*, *31*), and were injected with viral titres of 2.8×10^{13} vg/mL for AAV9-hSyn1-DIO-oChIEF-Citrine and 1.4×10^{13} vg/mL for AAV9-TRE_{3G}-Cre.

Drugs and peptides

Anisomycin (Sigma Aldrich Japan Co., Tokyo, Japan) was dissolved in a minimum quantity of HCl, diluted with phosphate buffered saline (PBS), and adjusted to pH 7.4 with NaOH. The Tat-beclin 1 peptide D-amino acid sequence (RRRQRRKKRGYGGTGFEGDHWIEFTANFVNT; synthesized by GenScript through Funakoshi Co., Ltd., Tokyo, Japan) was dissolved in either PBS (tat-beclin) or anisomycin solution (anisomycin + tat-beclin). Drugs and peptides were aliquoted into single experiment volumes and stored at −80°C.

Surgery

Mice were 10–12 weeks old at the time of surgery. They were anesthetized with isoflurane, given an intraperitoneal injection of pentobarbital solution (80 mg/kg of body weight), and then placed in a stereotactic apparatus (Narishige, Tokyo, Japan). Virus (500 nL) was injected at 100 nL min^{-1} bilaterally into the AC (−2.7 mm anteroposterior [AP], ±4.4 mm mediolateral [ML], +3.3 mm dorsoventral [DV]), MGm (−3.1 mm AP, ±1.9 mm ML, +3.5 mm DV), and LA (−1.7 mm

AP, ±3.4 mm ML, +4.1 mm DV). After injection, the injection cannula was kept in place for 5 min before its withdrawal, then a stainless guide cannula (PlasticsOne, Roanoke, VA, USA) targeting the LA was positioned 3.1 mm ventral to the bregma and fixed on the skull with dental cement. A dummy cannula (PlasticsOne) with a cap was then inserted into the guide cannula. Mice were allowed to recover for at least 7 days in individual home cages before starting the experiments. All drug infusions were performed under isoflurane anaesthesia, using an injection cannula with a 0.25 mm internal diameter (PlasticsOne), and extending beyond the end of the guide cannula by 1 mm. Immediately after retrieval, 0.5 µL of drug solution was injected bilaterally (total: 1 µL/mouse) into the LA at a flow rate of 0.2 µL/min. Following drug infusion, the injection cannula was left for 2 min to allow for drug diffusion. In all experiments, 1 µL of drug solution contained either PBS, 125 µg of anisomycin, or 125 µg of anisomycin + 20 µg of tat-beclin.

Auditory fear conditioning (AFC)

All behavioural sessions were conducted during the light cycle, in a dedicated soundproof behavioural room (Yamaha Co., Shizuoka, Japan), described here as Room A. Different chambers were used for each AFC session. All chambers were different in shape, lighting pattern, and floor texture. After recovery from surgery, a maximum of six mice were moved from their home cages on racks in the maintenance room to a soundproof waiting room (Yamaha Co.). Mice were left undisturbed for at least 15 min before and after each session, and during the experiment. In each session, one mouse in its home cage was moved into Room A. The experiments were performed on AAV-injected c-fos-tTA mice, maintained on food containing 40 mg/kg doxycycline (DOX).

Habituation. Three–four weeks after virus infection, mice were allowed to explore the context for 2 min before exposure to a neutral tone (30 sec, 65 dB, 2 kHz). The mice then remained for an additional 2.5 min before being returned to their home cages. After the second habituation session, DOX was removed and the mice were maintained on normal food. Habituation was done with tone presentation to decrease the startle response to any tone presentation in the subsequent sessions.

Conditioning. Two days later, mice were placed in the context for 2 min, and then received a single presentation of a conditioned tone (30 sec, 65 dB, 7 kHz), co-terminating with a shock (2 sec, 0.4 mA); mice remained for 30 sec, and were then returned to their home cages. Six hours later, the food was changed to one containing 1000 mg/kg DOX.

Testing. Mice were allowed to explore the unfamiliar context for 2 min before receiving the test tone (30 sec, 65 dB, 7 or 2 kHz), then 30 sec later they were returned to their home cages, except in the test 1 condition, where they were subjected to isoflurane anaesthesia and drug infusion.

Optogenetic stimulation (10 and 20 Hz). For the placement of two branch-type optical fibres (internal diameter, 0.25 mm) connected to a housing with a cap, mice were anaesthetized with approximately 2.0% isoflurane and the optic fibres were inserted into guide cannulas. The tip of the optical fibre was targeted 0.5 mm above the LA (DV 3.6 mm from the bregma). Mice with the inserted optic fibres were then returned to their home cages and left for at least 2 h. The fibre unit-connected mouse was attached to an optical swivel, which was connected to a laser unit (8–10 mW, 473 nm). The delivery of light was controlled using a schedule stimulator in time-lapse mode. The optogenetic session was 9 min in duration, and consisted of three 3 min epochs, with the first and third being Light-Off epochs, and the second being a Light-On epoch. During the Light-On epoch, mice received optical stimulation (10 or 20 Hz, 15 ms pulse width) for the entire

3 min. One hour after the end of the session, the fibre was removed from the cannula under anaesthesia.

***In vivo* LTP induction**. Immediately after test 4, mice were placed in a different home cage, and after being allowed 2 min for exploration, optical LTP was induced with 10 trains of light (each train consisted of 100 pulses of light, 5 ms each, at 100 Hz) at 90 sec inter-train intervals.

Experiments consisting of two overlapping memories (Figs. 3, 4, S5 and S6)

Habituation, testing, and optogenetic stimulation sessions were as described above.

Conditioning. After 2 days OFF DOX, mice were fear conditioned to a 7 kHz tone as described above. Immediately after the session, mice were put back on food containing 1000 mg/kg DOX. One hour later, mice were injected intraperitoneally with doxycycline hyclate (120 mg/kg) to stop the expression of oChIEF. Five or twenty-four hours after the 7 kHz fear conditioning, mice were exposed to 2 kHz fear conditioning.

***In vivo* LTP or LTD induction**. Immediately after the test session, optical LTP or LTD was applied. Optical LTP was induced with 10 trains of light (each train consisted of 100 pulses of light, 5 ms each, at 100 Hz) at 90 sec inter-train intervals. Optical LTD was induced with 900 pulses of light, 2 ms each, at 1 Hz.

Two tone discrimination experiment (Fig. S1)

Naive male C57BL/6J mice were used. Mice were exposed to the above-mentioned protocol during the habituation and conditioning sessions. One day after conditioning, mice were divided into two groups, the first of which was tested with the 7 kHz tone first, and was then tested with the 2 kHz tone on the following day, and the second of which was tested with the 2 kHz tone first, and was then tested with the 7 kHz tone. During test sessions, mice were allowed to explore the unfamiliar context for 2 min before receiving the testing tone, and then 30 sec later, the mice were returned to their home cages.

Behavioural analysis

All experiments were conducted using a video tracking system (Muromachi Kikai, Tokyo, Japan) to measure the freezing behaviour of the animals. Freezing was defined as a complete absence of movement, except for respiration. Scoring of the duration of the freezing response was started after 1 sec of sustained freezing behaviour. All behavioural sessions were digitally recorded using Bandicam software (Bandisoft, Seoul, Korea). Animals were excluded when the virus or the cannula was not in the target position.

In vivo LTP or LTD induction (Figs. 1 and 4)

For behavioural experiments, optical LTP was induced with 10 trains of light (each train consisted of 100 pulses of light, 5 ms each, at 100 Hz) at 90 sec inter-train intervals. Optical LTD was induced with 900 pulses of light, 2 ms each, at 1 Hz. For the LTP occlusion experiment, optical LTP was induced with five trains of light (each train consisted of 100 pulses of light, 5 ms each, at 100 Hz) at 3 min inter-train intervals.

In vivo recording (Fig. 2 and S3)

Four weeks after the injection of AAV viral vectors into the MGm and AC, mice were anesthetized with pentobarbital and mounted on a stereotaxic frame. An optic fibre was glued to the recording tungsten electrode so that the tip of the fibre was 500 μm above the tip of the

electrode. The optrode was inserted into the LA, and the optic fibre was connected to a 473 nm laser unit. The LTP or LTD induction protocol was identical to that used in the behavioural test. After establishing a stable baseline at the recording site for 20 min (stimulation frequency of 0.033 Hz), *in vivo* LTP or LTD was optically induced, which was followed by at least 20 min of 0.033 Hz stimulation. Data were analysed using Clampex 10.7 software. All animals were perfused after the recordings, and the positions of the recording sites were verified.

LTP occlusion experiment

The behavioural part of this experiment was performed as described above. One day after the test session and drug infusion, mice were anesthetized and the guide cannulas with dental cement were removed from the skull. *In vivo* recording was then performed as described above.

Immunohistochemistry

One and a half hours after the desired session, the mice were deeply anesthetized with pentobarbital solution and perfused transcardially with PBS (pH 7.4) followed by 4% paraformaldehyde in PBS (PFA). The brains were removed, further post-fixed by immersion in PFA for 12–18 h at 4°C, equilibrated in 25% sucrose in PBS for 36–48 h at 4°C, and then stored at –80°C. Brains were cut into 50 μm coronal sections using a cryostat and transferred to 12-well cell culture plates (Corning, NY, USA) containing PBS. After washing with PBS, the floating sections were treated with blocking buffer (3% normal donkey serum; S30, Chemicon by EMD Millipore, Billerica, MA, USA) in PBS containing 0.2% Triton X-100 and 0.05% tween 20 (PBST), at room temperature for 1 h. The following primary antibodies were applied in blocking buffer at 4°C for 24–36 h: rat anti-GFP (1:1000, Nacalai Tesque, 04404-84, GF090R), rabbit anti-c-Fos (1:1000, Santa Cruz Biotechnology, sc-7202), goat anti-c-Fos (1:1000, Santa Cruz Biotechnology, sc-52-G), and rabbit anti-mCherry (1:1000, Clontech, 632496). After three 10 min washes with 0.2% PBST, sections were incubated in blocking buffer at room temperature for 2–3 h, with the following corresponding secondary antibodies: donkey anti-rat IgG Alexa Fluor 488 (1:1000, Molecular Probes, A21208), donkey anti-rabbit IgG Alexa Fluor 546 (1:1000, Molecular Probes, A10040), or donkey anti-goat IgG Alexa Fluor 647 (1:1000, Molecular Probes, A21447). Finally, the sections were treated with DAPI (1 μg/mL, Roche Diagnostics, 10236276001) and then washed with 0.2% PBST three times for 10 min each before being mounted onto glass slides with ProLong Gold antifade reagent (Invitrogen).

Confocal microscopy and cell counting

Images were acquired using a Zeiss LSM 780 confocal microscope (Carl Zeiss, Jena, Germany) with a 20× plan apochromat objective lens. All acquisition parameters were kept constant within each magnification. To quantify the number of each immunoreactive cell type in the target regions after collecting z-stacks (approximately 10 optical sections of 10 μm thickness), three coronal sections per mouse (n = 4 mice) were manually counted. Overlaps between the GFP^+ and $c\text{-}fos^+$ cells, as well as $mCherry^+$ and $c\text{-}fos^+$ cells, were manually counted. Chance level was calculated by multiplying % $mCherry^+$ / DAPI by % $c\text{-}fos^+$ / DAPI.

Statistics

Statistical analyses were performed using Prism 6.01 (GraphPad Software, San Diego, CA, USA). Data from two groups were compared using two-tailed unpaired Student's *t*-tests. Multiple-

group comparisons were assessed using ANOVA with post hoc tests as described in the appropriate figure legend. Quantitative data are presented as mean ± s.e.m.

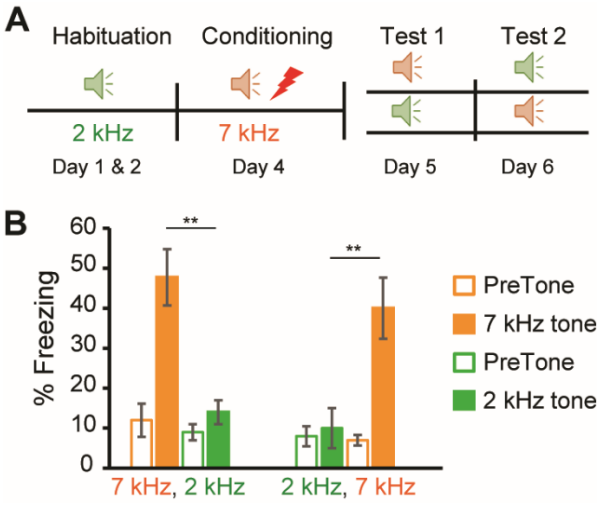

Fig. S1. Mice discriminate between 2 kHz and 7 kHz tones.

(**A**) Design for the discrimination experiment. Wild-type mice were exposed to AFC and then divided into two groups; the first one received a 7 kHz tone in test 1 and a 2 kHz tone in test 2, while the second group received the tones in the opposite order. (**B**) Freezing levels before and during the two tones (n = 11 mice/group). Statistical comparisons were performed using a paired t-test. * $P < 0.05$; ** $P < 0.01$. Data are represented as mean ± SEM.

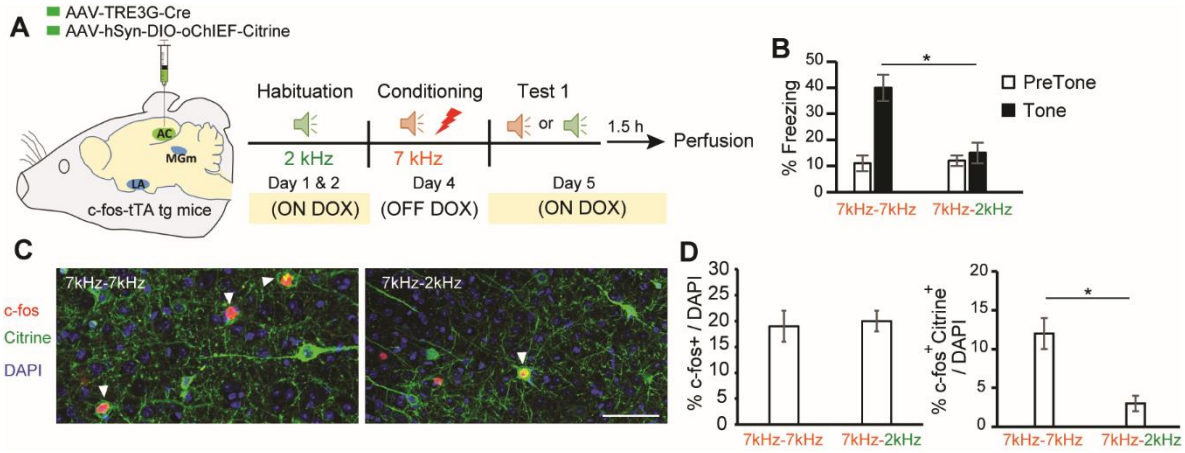

Fig. S2. 7 kHz and 2 kHz tones activate different neuronal ensembles in the AC.

(**A**) Experimental design to label the 7 kHz and 2 kHz-responsive ensembles in the AC with citrine and c-Fos antibodies, respectively. (**B**) Freezing levels before and during 7 kHz and 2 kHz tone presentations in test sessions. (**C**) Representative images showing two different ensembles encoding different tones. Arrow heads represent overlapping cells (c-Fos$^+$/citrine$^+$ overlap). Scale bars, 50 μm. (**D**) Left, c-Fos$^+$ neurons activated during test session. Right, c-Fos$^+$/citrine$^+$ overlap cell counts (n = 4 mice/group). Statistical comparisons were performed using an unpaired t-test. * $P < 0.05$. Data are represented as mean ± SEM.

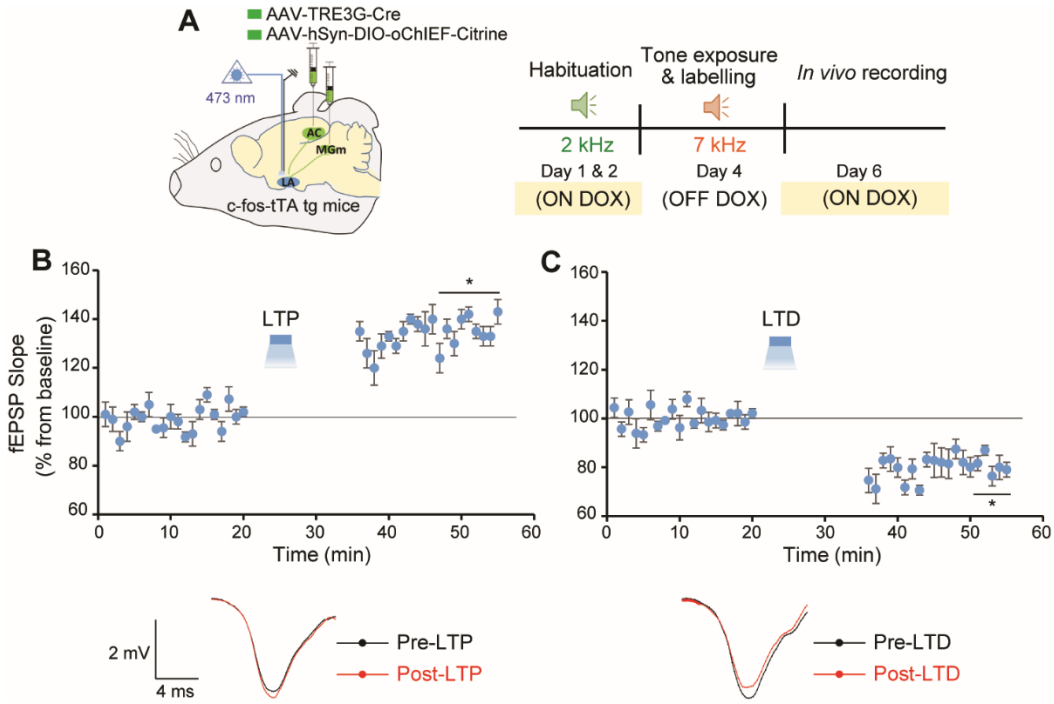

Fig. S3. *In vivo* induction of optical LTP and LTD.

(**A**) Experimental design. (**B**) Top, average of *in vivo* field EPSP slope (normalized to baseline) before and after LTP induction (n = 4 mice/group). Bottom, representative traces before (black) and after (red) the stimulation protocol. (**C**) Top, average of *in vivo* field EPSP slope (normalized to baseline) before and after LTD induction (n = 4 mice/group). Bottom, representative traces before (black) and after (red) the stimulation protocol. Statistical comparisons were performed using two-way repeated measures ANOVA. * $P < 0.05$. Data are represented as mean ± SEM.

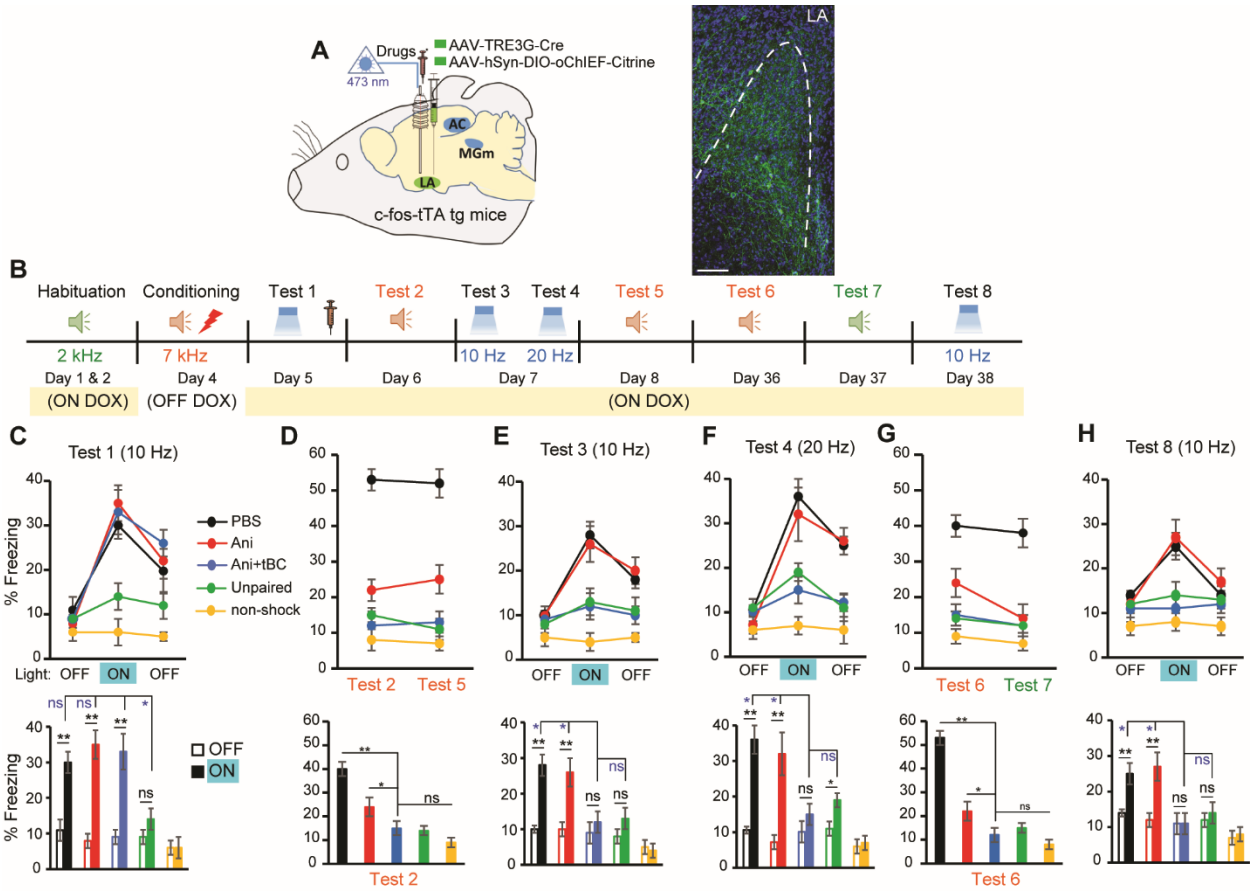

Fig. S4. LA engram cells no longer store the memory after complete amnesia.

(**A**) Left, labelling strategy for the AFC-responsive ensemble in LA using the c-Fos/TetTag system. Right, expression of oChIEF in LA neurons. Dashed line shows the border of LA. Scale bar, 100 μm. (**B**) Experimental design for erasure of the memory engram. (**C** to **H**) Top, freezing levels during fear memory recall by 10 Hz stimulation (**C**), in response to the conditioned tone (**D**), during 10 Hz stimulation (**E**), during 20 Hz stimulation (**F**), in response to the conditioned tone and neutral tone at a remote time point (**G**), and during 10 Hz stimulation at a remote time point (**H**). Bottom, statistical significance between groups (n = 10 mice/group). Statistical comparisons were performed using one-way ANOVA (**D** and **G**) and two-way ANOVA (**C**, **E**, **F** and **H**). Ani, anisomycin; tBC, tat-beclin. * $P < 0.05$; ** $P < 0.01$. Data are represented as mean ± SEM.

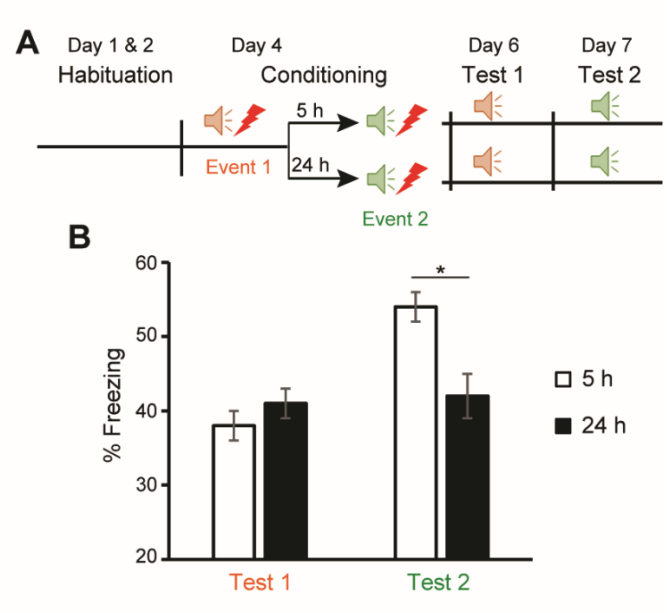

Fig. S5. Memory enhancement after encoding two memories 5 hours apart.

(**A**) Design for the memory linking experiment. Wild-type mice were exposed to event 1 (7 kHz + shock) and then divided into two groups. The first group was exposed to event 2 (2 kHz + shock) 5 h after being exposed to event 1, while the second group was exposed to event 2 after 24 h. Both groups received a 7 kHz tone in test 1, while they received a 2 kHz tone in test 2. (**B**) Freezing levels of both groups in tests 1 and 2 ($n = 6$ mice/group). Statistical comparisons were performed using an unpaired *t*-test. * $P < 0.05$. Data are represented as mean ± SEM.

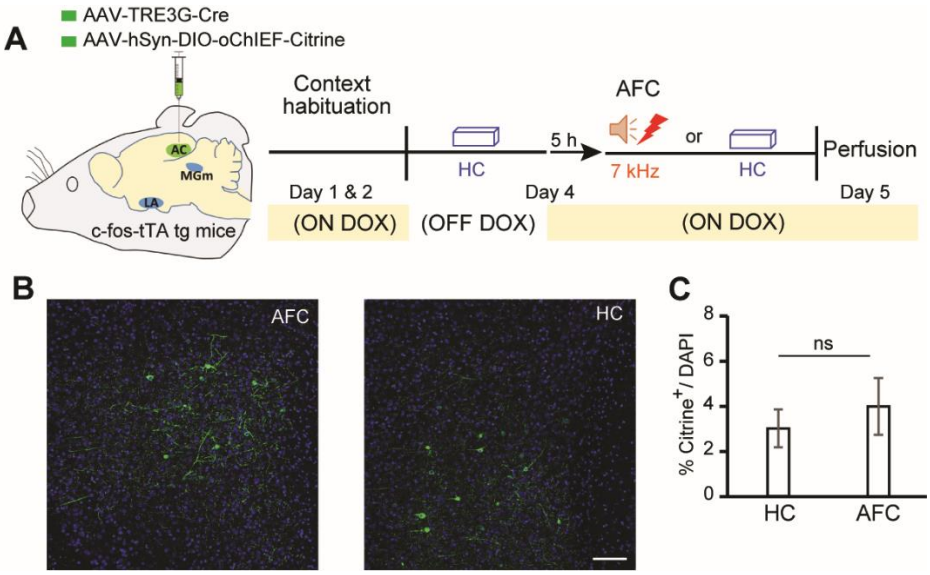

Fig. S6. Five hours ON DOX is enough to stop the expression of oChIEF.

(**A**) Experimental design. After 2 days without DOX in their food, mice were put back on DOX for 5 h, and were then either exposed to AFC or stayed in their home cage (HC). One day later, they were perfused. (**B**) Representative images showing oChIEF-citrine expression in AC after AFC while mice were ON DOX chow (1 g kg^{-1}). Scale bar, 100 µm. (**C**) oChIEF-citrine cell counts (unpaired *t*-test, $n = 4$ mice/group). * $P < 0.05$. Data are represented as mean ± SEM.

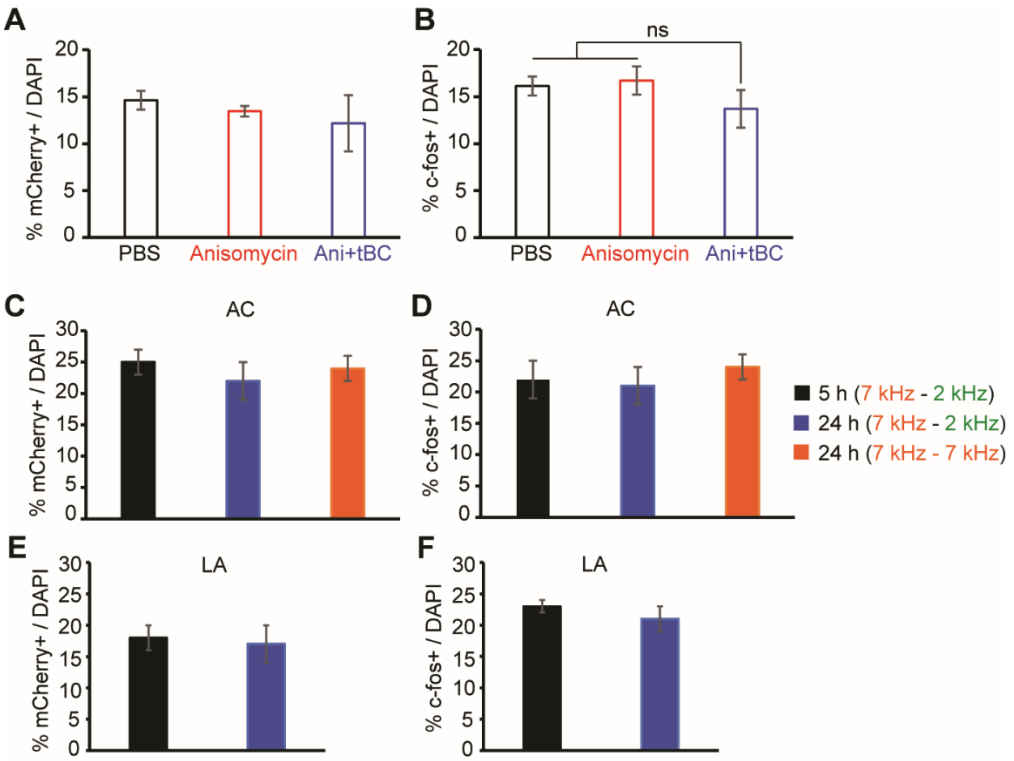

Fig. S7. Efficiency of engram labelling was similar across groups.

(**A** and **B**) Related to figure 2, E to I. (**A**) Counts for mCherry^{+} neurons which activated during 7 kHz fear conditioning. (**B**) Counts for c-Fos^{+} neurons which activated in response to 10Hz optogenetic stimulation. (**C** to **F**) Related to figure 3, A to E. (**C** and **E**) Counts for mCherry^{+} neurons which activated during 7 kHz fear conditioning in AC (**C**) and in LA (**E**). (**D** and **F**) Counts for c-Fos+ neurons in AC (**D**) and in LA (**F**). Data are represented as mean ± SEM.

References and Notes

1. T. V. Bliss, G. L. Collingridge, A synaptic model of memory: Long-term potentiation in the hippocampus. *Nature* **361**, 31–39 (1993). doi:10.1038/361031a0 Medline

2. T. V. Bliss, T. Lomo, Long-lasting potentiation of synaptic transmission in the dentate area of the anaesthetized rabbit following stimulation of the perforant path. *J. Physiol.* **232**, 331–356 (1973). doi:10.1113/jphysiol.1973.sp010273 Medline

3. M. Bocchio, S. Nabavi, M. Capogna, Synaptic Plasticity, Engrams, and Network Oscillations in Amygdala Circuits for Storage and Retrieval of Emotional Memories. *Neuron* **94**, 731–743 (2017). doi:10.1016/j.neuron.2017.03.022 Medline

4. J. P. Johansen, C. K. Cain, L. E. Ostroff, J. E. LeDoux, Molecular mechanisms of fear learning and memory. *Cell* **147**, 509–524 (2011). doi:10.1016/j.cell.2011.10.009 Medline

5. S. Nabavi, R. Fox, C. D. Proulx, J. Y. Lin, R. Y. Tsien, R. Malinow, Engineering a memory with LTD and LTP. *Nature* **511**, 348–352 (2014). doi:10.1038/nature13294 Medline

6. G. Neves, S. F. Cooke, T. V. Bliss, Synaptic plasticity, memory and the hippocampus: A neural network approach to causality. *Nat. Rev. Neurosci.* **9**, 65–75 (2008). doi:10.1038/nrn2303 Medline

7. S. Tonegawa, M. Pignatelli, D. S. Roy, T. J. Ryan, Memory engram storage and retrieval. *Curr. Opin. Neurobiol.* **35**, 101–109 (2015). doi:10.1016/j.conb.2015.07.009 Medline

8. J. H. Han, S. A. Kushner, A. P. Yiu, H.-L. Hsiang, T. Buch, A. Waisman, B. Bontempi, R. L. Neve, P. W. Frankland, S. A. Josselyn, Selective erasure of a fear memory. *Science* **323**, 1492–1496 (2009). doi:10.1126/science.1164139 Medline

9. S. A. Josselyn, S. Köhler, P. W. Frankland, Finding the engram. *Nat. Rev. Neurosci.* **16**, 521–534 (2015). doi:10.1038/nrn4000 Medline

10. X. Liu, S. Ramirez, P. T. Pang, C. B. Puryear, A. Govindarajan, K. Deisseroth, S. Tonegawa, Optogenetic stimulation of a hippocampal engram activates fear memory recall. *Nature* **484**, 381–385 (2012). Medline

11. L. G. Reijmers, B. L. Perkins, N. Matsuo, M. Mayford, Localization of a stable neural correlate of associative memory. *Science* **317**, 1230–1233 (2007). doi:10.1126/science.1143839 Medline

12. A. J. Silva, Y. Zhou, T. Rogerson, J. Shobe, J. Balaji, Molecular and cellular approaches to memory allocation in neural circuits. *Science* **326**, 391–395 (2009). doi:10.1126/science.1174519 Medline

13. S. Tonegawa, X. Liu, S. Ramirez, R. Redondo, Memory Engram Cells Have Come of Age. *Neuron* **87**, 918–931 (2015). doi:10.1016/j.neuron.2015.08.002 Medline

14. D. J. Cai, D. Aharoni, T. Shuman, J. Shobe, J. Biane, W. Song, B. Wei, M. Veshkini, M. La-Vu, J. Lou, S. E. Flores, I. Kim, Y. Sano, M. Zhou, K. Baumgaertel, A. Lavi, M. Kamata, M. Tuszynski, M. Mayford, P. Golshani, A. J. Silva, A shared neural ensemble links distinct contextual memories encoded close in time. *Nature* **534**, 115–118 (2016). doi:10.1038/nature17955 Medline

15. M. Nomoto, N. Ohkawa, H. Nishizono, J. Yokose, A. Suzuki, M. Matsuo, S. Tsujimura, Y. Takahashi, M. Nagase, A. M. Watabe, F. Kato, K. Inokuchi, Cellular tagging as a neural network mechanism for behavioural tagging. *Nat. Commun.* **7**, 12319 (2016). doi:10.1038/ncomms12319 Medline

16. N. Ohkawa, Y. Saitoh, A. Suzuki, S. Tsujimura, E. Murayama, S. Kosugi, H. Nishizono, M. Matsuo, Y. Takahashi, M. Nagase, Y. K. Sugimura, A. M. Watabe, F. Kato, K. Inokuchi, Artificial association of pre-stored information to generate a qualitatively new memory. *Cell Rep.* **11**, 261–269 (2015). doi:10.1016/j.celrep.2015.03.017 Medline

17. A. J. Rashid, C. Yan, V. Mercaldo, H.-L. Hsiang, S. Park, C. J. Cole, A. De Cristofaro, J. Yu, C. Ramakrishnan, S. Y. Lee, K. Deisseroth, P. W. Frankland, S. A. Josselyn, Competition between engrams influences fear memory formation and recall. *Science* **353**, 383–387 (2016). doi:10.1126/science.aaf0594 Medline

18. J. Yokose, R. Okubo-Suzuki, M. Nomoto, N. Ohkawa, H. Nishizono, A. Suzuki, M. Matsuo, S. Tsujimura, Y. Takahashi, M. Nagase, A. M. Watabe, M. Sasahara, F. Kato, K. Inokuchi, Overlapping memory trace indispensable for linking, but not recalling, individual memories. *Science* **355**, 398–403 (2017). doi:10.1126/science.aal2690 Medline

19. T. Rogerson, D. J. Cai, A. Frank, Y. Sano, J. Shobe, M. F. Lopez-Aranda, A. J. Silva, Synaptic tagging during memory allocation. *Nat. Rev. Neurosci.* **15**, 157–169 (2014). doi:10.1038/nrn3667 Medline

20. W. B. Kim, J.-H. Cho, Encoding of Discriminative Fear Memory by Input-Specific LTP in the Amygdala. *Neuron* **95**, 1129–1146.e5 (2017). doi:10.1016/j.neuron.2017.08.004 Medline

21. T. J. Ryan, D. S. Roy, M. Pignatelli, A. Arons, S. Tonegawa, Engram cells retain memory under retrograde amnesia. *Science* **348**, 1007–1013 (2015). doi:10.1126/science.aaa5542 Medline

22. P. Tovote, J. P. Fadok, A. Lüthi, Neuronal circuits for fear and anxiety. *Nat. Rev. Neurosci.* **16**, 317–331 (2015). doi:10.1038/nrn3945 Medline

23. M. Shehata, K. Inokuchi, Does autophagy work in synaptic plasticity and memory? *Rev. Neurosci.* **25**, 543–557 (2014). doi:10.1515/revneuro-2014-0002 Medline

24. M. Shehata, H. Matsumura, R. Okubo-Suzuki, N. Ohkawa, K. Inokuchi, Neuronal stimulation induces autophagy in hippocampal neurons that is involved in AMPA receptor degradation after chemical long-term depression. *J. Neurosci.* **32**, 10413–10422 (2012). doi:10.1523/JNEUROSCI.4533-11.2012 Medline

25. M. Shehata, K. Abdou, K. Choko, M. Matsuo, H. Nishizono, K. Inokuchi, Autophagy enhances memory erasure through synaptic destabilization. *J. Neurosci.* **38**, 3809–3822 (2018). doi:10.1523/JNEUROSCI.3505-17.2018 Medline

26. C. C. Huang, C. C. Chen, Y. C. Liang, K. S. Hsu, Long-term potentiation at excitatory synaptic inputs to the intercalated cell masses of the amygdala. *Int. J. Neuropsychopharmacol.* **17**, 1233–1242 (2014). doi:10.1017/S1461145714000133 Medline

27. S. Park, J. Lee, K. Park, J. Kim, B. Song, I. Hong, J. Kim, S. Lee, S. Choi, Sound tuning of amygdala plasticity in auditory fear conditioning. *Sci. Rep.* **6**, 31069 (2016). doi:10.1038/srep31069 Medline

28. E. Tsvetkov, W. A. Carlezon Jr., F. M. Benes, E. R. Kandel, V. Y. Bolshakov, Fear conditioning occludes LTP-induced presynaptic enhancement of synaptic transmission in the cortical pathway to the lateral amygdala. *Neuron* **34**, 289–300 (2002). doi:10.1016/S0896-6273(02)00645-1 Medline

29. T. Abe, H. Kiyonari, G. Shioi, K. Inoue, K. Nakao, S. Aizawa, T. Fujimori, Establishment of conditional reporter mouse lines at ROSA26 locus for live cell imaging. *Genesis* **49**, 579–590 (2011). doi:10.1002/dvg.20753 Medline

30. A. Iida, N. Takino, H. Miyauchi, K. Shimazaki, S. Muramatsu, Systemic delivery of tyrosine-mutant AAV vectors results in robust transduction of neurons in adult mice. *BioMed Res. Int.* **2013**, 974819 (2013). doi:10.1155/2013/974819 Medline

31. X. G. Li, T. Okada, M. Kodera, Y. Nara, N. Takino, C. Muramatsu, K. Ikeguchi, F. Urano, H. Ichinose, D. Metzger, P. Chambon, I. Nakano, K. Ozawa, S. Muramatsu, Viral-mediated temporally controlled dopamine production in a rat model of Parkinson disease. *Mol. Ther.* **13**, 160–166 (2006). doi:10.1016/j.ymthe.2005.08.009 Medline